M. D. Radmilović-Radjenović, *et al.*: Study of Multipactor Effect with ...
Nuclear Technology & Radiation Protection: Year 2017, Vol. 32, No. 2, pp. 115-119

115

STUDY OF MULTIPACTOR EFFECT WITH APPLICATIONS TO SUPERCONDUCTIVE RADIOFREQUENCY CAVITIES

by

Marija D. RADMILOVIĆ-RADJENOVIĆ [1], Petar D. BELIČEV [2] *, and Branislav M. RADJENOVIĆ [1]

[1] Institute of Physics, University of Belgrade, Belgrade, Serbia
[2] Vinča Institute of Nuclear Sciences, University of Belgrade, Belgrade, Serbia

In this paper a one-dimensional Particle-in-Cell/Monte Carlo collision code has been used in order to study characteristics of multipactors. For multipactor to occur each electron striking the surface must generate more than one secondary on average. The ratio of primary to secondary electrons is given by the secondary emission yield. For this study, calculations were carried out by using Sternglass model that includes energy dependence of the secondary emission yield. The obtained simulation results for the pressure dependence of the breakdown time follow the scaling law. Number of electrons increases in time, while their mean energy decreases. Since secondary electron emission at the cavity surface plays an important role, simulation results, presented here, can help cavity designers predict multipacting issues before fabrication.

Key words: RF cavitie, multipactor effect, secondary electron emission

INTRODUCTION

Studies of the secondary emission process, which is still believed to be one of the critical contributors to multipactor discharge phenomenon, are important in designing room temperature or superconductive radiofrequency (SRF) cavities of linear accelerators (see fig.1), storage rings, and free electron lasers [1, 2]. Multipactor is a resonant electron instability where an electron striking the surface with a given energy, produces more than one secondary particle [3-5]. If the secondary electrons are returned to the surface at the same radio-frequency (RF) phase and energy as the primary ones, then an exponential growth in electron number will take place. These electrons may absorb all additional RF power from the cavity, preventing it from increasing the voltage.

Since multipactor is an undesirable effect, the prediction of the RF input power threshold of a specific RF component is a very important task. It depends basically on: component's geometry, type of material, gap size, and amplitude and frequency of the electric field [6]. For high gradient accelerators, RF voltage breakdown is one of the major factors which imposes the limits on the maximum field gradient. Most of the theoretical studies of the multipactors are based on a one-dimensional model with a spatially

uniform approximation of the electromagnetic field [7-9]. However, many common RF devices involve structures where the field is inhomogeneous, where breakdown predictions based on such simple models will not be reliable.

It was shown that multipacting could be overcome by changing the cavity cross-section from a rectangular to a spherical or elliptical shape, as shown in fig. 2. In the rectangular cavity, the electrons return to the same point from which they were emitted, where they can cause secondary emission. In the elliptical cavity, however, the emitted electrons drift towards the cavity equator, where the electric field is not strong enough for secondary emission to persist.

Multipaction breakdown is due to a resonant-secondary-electron emission in the conductor wall under high-vacuum condition, when the mean free path of an electron is greater than the distance between the inner and outer conductors. Under such conditions, free electrons are accelerated by the electric field and upon striking the conductor surface produce secondary electrons. Transitions from classical discharge to multipactor in RF range takes place at lower pressures as depicted in fig. 3.

In this study, one-dimensional electrostatic particle-in-cell simulation (PIC) method coupled with Monte-Carlo (MC) collision model has been employed [10]. The formation of multipactor is strongly

---

116

M. D. Radmilović-Radjenović, *et al*.: Study of Multipactor Effect with ...
Nuclear Technology & Radiation Protection: Year 2017, Vol. 32, No. 2, pp. 115-119
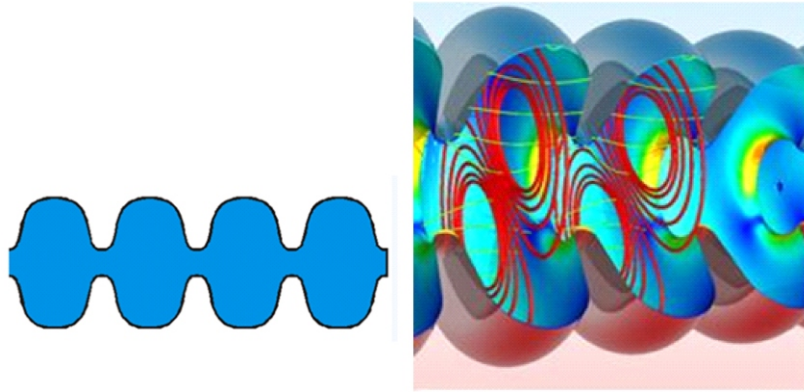
Figure 1. Schematic view (left) and cut (right) of the superconductive radiofrequency (SRF) cavities
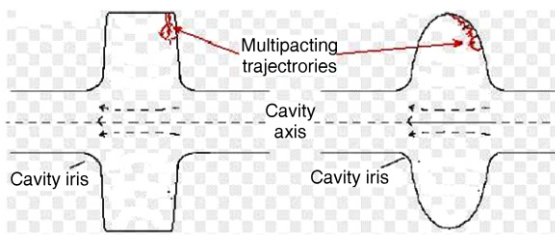

Figure 2. Multipacting trajectories when the cavity cross-section has a rectangular (left) and elliptical shape (right)
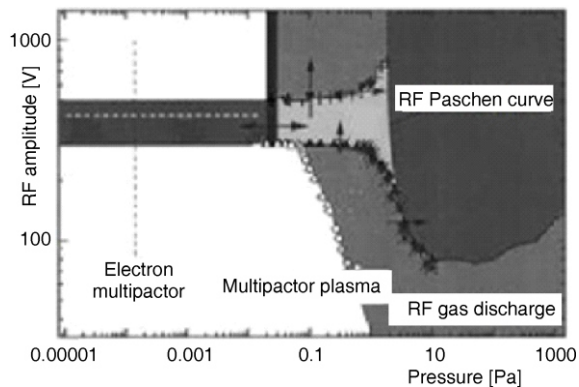

Figure 3. Transition region from the gas discharge to multipactor discharges [9]

dependent upon the secondary electron yield (SEY) of a surface. In the PIC/MCC code we have implemented the Sternglass formula as a standard description for the yield of secondary electrons, as a function of incident electron energy. Calculations were performed for argon gas at the low pressures. A good agreement between the obtained simulation results and the scaling law [11] for the breakdown time confirmed that Particle-in-cell technique could be used for modelling multipactors. For the future work, calculations should be extended to other SEY models.

SIMULATION TECHNIQUE

The simulation code extensively used in this study is one-dimensional bounded electrostatic PIC code with MC treatment of collisional processes. Since PIC codes have been well documented in nu-merous publications [12, 13] we shall provide only a brief description.

In PIC simulations, the so-called superparticles move in the discharge space through an artificial grid on a time step basis. At the beginning of the simulation, superparticles are distributed in the simulation domain. A self-consistent potential distribution is determined from the superparticles positions and the externally applied voltage by weighting the particles to the grid points and solving Poisson's equation. The simulation proceeds by calculating the electric field and weighting it to the particle positions. Then, the force exerted by the electric field is computed and particle velocities and positions are updated.

Collisional processes are accounted for by using the null-collision method. For each type of projectile a total collision probability is determined as

$$P_t = 1 - \exp(-\nu_{max}\Delta t) \qquad (1)$$

with maximum collision frequency is given by

$$\nu_{max} = N_g \max_{\varepsilon}[\sigma_t(\varepsilon)\upsilon(\varepsilon)] \qquad (2)$$

where N_g is spatially uniform target density, $\upsilon(\varepsilon)$ – the incident speed of a particle with energy ε and Δt – the time interval. The total cross-section $\sigma_t(\varepsilon)$ could be found by summation over all processes j

$$\sigma_t(\varepsilon) = \sum_j \sigma_j(\varepsilon) \qquad (3)$$

Choices of boundary conditions depend on the physical conditions of the boundary walls and electrodes. When an electron reaches the boundary, it is assumed to be absorbed. The electron impact secondary emission may be represented by the secondary emission coefficient that is equal to the flux of the emitted electrons normalized to the initial flux [14]. In this study we performed PIC/MCC calculations by using the energy dependence model of secondary electron production proposed by Sternglass [15].

Sternglass model

The implemented Sternglass model of the secondary emission coefficient is depicted in fig. 4. This

model includes energy dependence of the secondary emission coefficient given by [15-17]

$$\frac{\delta}{\delta_m} \quad (2.72)^2 \frac{\varepsilon_p}{\varepsilon_{p_m}} e^{2 \left[\frac{\varepsilon_p}{\varepsilon_{p_m}}\right]^{1/2}} \qquad (4)$$

where ε_p is the impact energy of the electron, and ε_{p_m} – the energy that corresponds to the the peak emission value of the secondary emission coefficient δ_m. Both quantities can be determined by fitting to the experimental data.

RESULTS

Figure 5 shows the dependence of the breakdown time on the gas pressure, defined implicitly by $N(\tau)/N(0) = 10^8$. Calculations were performed for argon as a feeling gas for the pressure from 0.005 Torr to 0.8 Torr*. The symbols represent the PIC/MCC results obtained by using the Sternglass model, while dot line corresponds to the prediction achieved by the scaling law for argon: $\tau \sim 64/p$ (where pressure p is expressed in Torr, while the breakdown time τ is expressed in nanoseconds) [11]. As can be observed, simulation results follow the scaling law [11].

PIC/MCC results for the time dependence of the number of particles are shown in fig. 6, obtained for the pressure of 8 mTorr. The number of electrons (solid curve) oscillates but increases in time. The number of ions (dash curve) also increases although it is much lower than the number of electrons, even at their minima. This behaviour clearly shows that the secondary electron emission is still the dominant mechanism over collisional ionization.

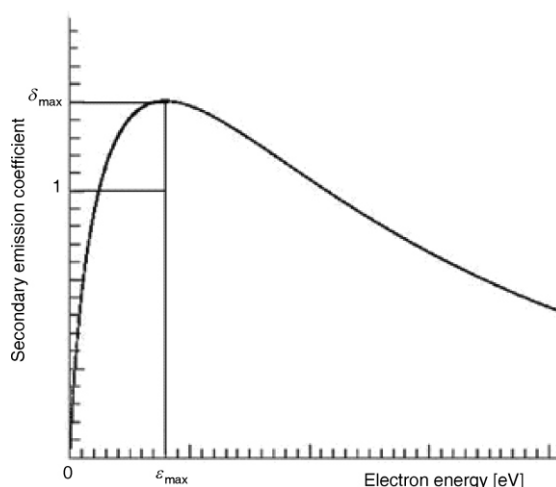Electrons in the multipactor discharge gain their energy by being accelerated by the RF electric field

Figure 4. The energy dependence of the secondary emission yield according to Sternglass model [11]
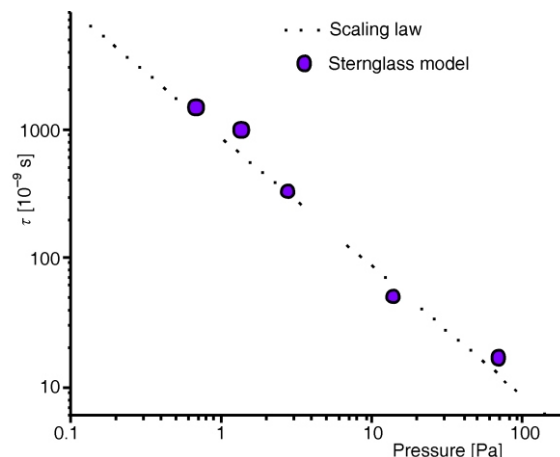
---
* 1 Torr = 133.32236 Pa

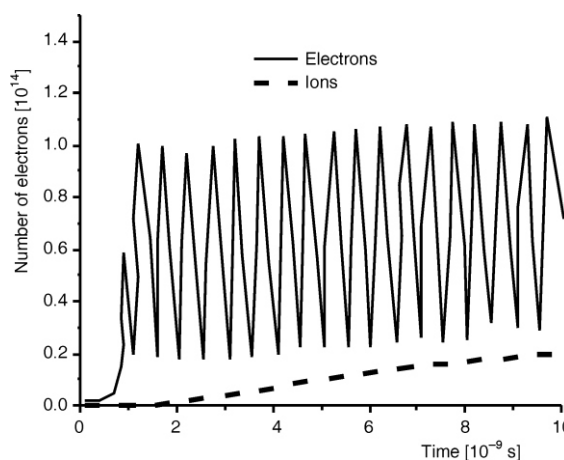**Figure 5. Breakdown time as a function of the gas pressure for argon**

Figure 6. Time dependence of the number of electrons (solid) and ions (dashed) in the argon gas at the pressure
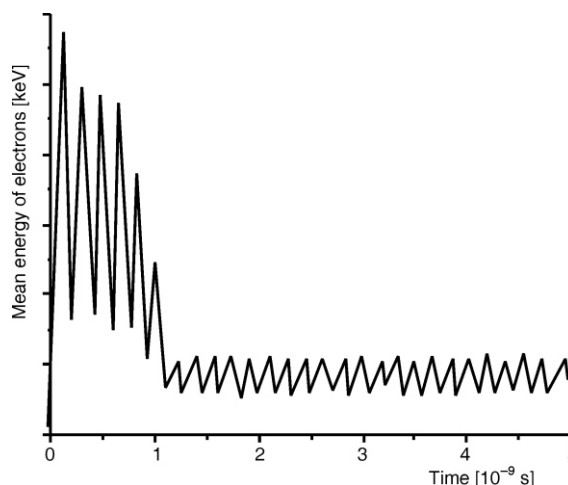
Figure 7. Average kinetic energy of electrons in the argon gas at the pressure of 8 mTorr

during the transit time. As can be seen from fig. 7, the average kinetic energy of electrons keeps decreasing.

Finally, the so called multipactor migration for TE10 mode, at the initial and the steady-state of the process, is shown in fig. 8. It can be seen that the multipactor starts in the edge regions, migrating to the central region as saturation is being achieved.
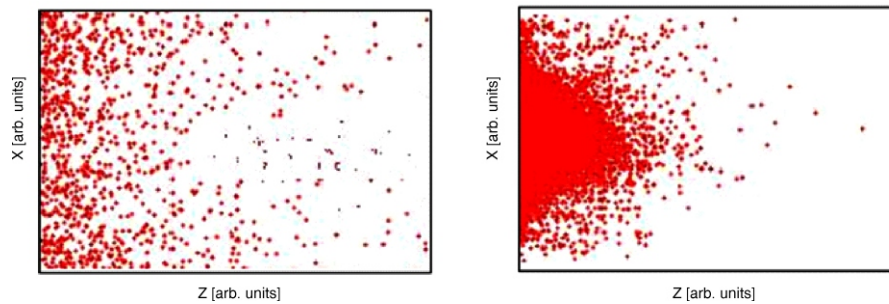
118

M. D. Radmilović-Radjenović, *et al.*: Study of Multipactor Effect with ...
Nuclear Technology & Radiation Protection: Year 2017, Vol. 32, No. 2, pp. 115-119

Figure 8. Multipactor migration for TE10 mode in the transient (left) and saturation (right)

CONCLUSIONS

In this paper a one-dimensional Particle-in-Cell/Monte Carlo collision code has been employed in order to study characteristics of multipactors. We performed calculations for for the dependence of the breakdown time on the gas pressure, the number of electrons and their energy as a function of time in argon at the low pressure. Simulation results were achieved by using Sternglas model for the energy dependence of the secondary emission coefficient. The obtained results for the breakdown time are in the line the scaling law. The number of electrons increases in time, while their energy decreases. The multipactor starts in the edge regions, and migrates to the central region as saturation is reached. It was found from the literature that simulation technique, especially PIC technique, represents very powerful tool for study of multipactors [18, 19]. Calculations should be extended for other SEY models, for example, proposed by Furman and Pivi [20]. This phenomenon is of considerable practical interest in the design and operation of radio frequency (RF) resonant structures.

ACKNOWLEDGEMENT

AUTHORS' CONTRIBUTIONS

The manuscript was written by M. D. Radmilović-Radjenović, B. M. Radjenović, and P. Beličev. Simulations were done by M. Radmilović-Radjenović, B. M. Radjenović, and P. Beličev. The figures were prepared by M. Radmilović-Radjenović.

REFERENCES

[1] Padamsee, H., RF Super Conductivity: Science, Technology and Applications, Wiley-VCH Verlag GmbH & Co. KGaA, Weinheim, Germany, 2009

[2] Hays, T., *et al.*, Handbook of Accelerator Physics and Engineering (Eds., A. W. Chao, M. Tigner), World Scientific Publishing Co., Singapore, 2002

[3] Vaughan, J. R. M., Multipactor, *IEEE-TED, 35* (1988), July, pp. 1172-1180

[4] Boni, R., *et al.*, Design and Operation of a Multipacting-Free 51.4 MHz rf Accelerating Cavity, *Nucl. Instrum. Methods A, 274* (1989), Jan.-Feb., pp. 49-55

[5] Udiljak, R., *et al.*, Multipactor in Low Pressure Gas, *Phys. Plasmas, 10* (2003), Oct., pp. 4105-4111

[6] Peter, W., *et al.*, Criteria for Vacuum Breakdown in RF Cavities, *IEEE Transactions on Nuclear Science, NS-30* (1983), Aug., pp. 3454-3456

[7] Kim, H., *et al.*, Modeling RF Window Breakdown: from Vacuum Multipactor to RF Plasma, *IEEE Trans. Dielectr. Electr. Insul., 14* (2007), Apr., pp. 766-773

[8] Semenov, V. E., *et al.*, Simulations of Multipactor Thresholds in Shielded Microstrip Lines, *J. Phys. D: Appl. Phys., 42* (2009), Sept., p. 205204, (7 pp)

[9] Hohn, F., *et al.*, The Transition of a Multipactor to a Low-Pressure Gas Discharge, *Physics of Plasmas, 4* (1997), Sept., pp. 940-944

[10] Verboncoeur, J. P., *et al.*, Simultaneous Potential and Circuit Solution for 1d Bounded Plasma Particle Simulation Codes, *Journal of Computational Physics, 104* (1993), 2, pp. 321-328

[11] Lau, Y. Y., *et al.*, Scaling Laws for Dielectric Window Breakdown in Vacuum and Collisional Regimes, *Appl. Phys. Lett., 89* (2006), 26, pp. 261-501

[12] Verboncoeur, J. P., Particle Simulation of Plasmas: Review and Advances, *Plasma Physics and Controlled Fusion, 47* (2005), 5A, pp. A231-A260

[13] Kim, H. C., Verboncoeur, J. P., Time-Dependent Physics of a Single-Surface Multipactor Discharge, *Phys. Plasmas, 12* (2005), Dec., p. 123504

[14] Vaughan, J. R. M., 1989 A New Formula for Secondary Emission Yield, *IEEE Trans. Electron Devices, 36* (1989), Sept., pp. 1963-1967

[15] Holliday, J. E., Sternglass, E. J., New Method for Range Measurements of Low-Energy Electrons in Solids, *J. Appl. Phys., 30* (1959), June, pp. 1428-1431

[16] Smith, H. B., *et al.*, Breakdown Behavior in Radio-Frequency Argon Discharges, *Physics of Plasmas, 10* (2003), Mar., pp. 875-881

[17] Deca, J., *et al.*, Spacecraft Charging Analysis with the Implicit Particle-ic-Cell Code iPic3D, *Physics of Plasmas, 20* (2013), Oct., p. 2902

[18] Sorolla, E., Sounas, A., Mattes, M., Space Charge Effects for Multipactor in Coaxial Lines, *Physics of Plasmas, 22* (2015), Mar., p. 033512

[19] Lin, S., *et al.*, Multipactor Threshold Calculation of Coaxial Transmission Lines in Microwave Applications with Nonstationary Statistical Theory, *Physics of Plasmas, 22* (2015), Aug., p. 082114

[20] Furman, M. A., Pivi, M. T. F., Probabilistic Model for the Simulation of secondary Electron Emission, *Physical Review Special Topics – Accelerators and Beams, 5* (2002), June, p. 124404

M. D. Radmilović-Radjenović, *et al*.: Study of Multipactor Effect with ...
Nuclear Technology & Radiation Protection: Year 2017, Vol. 32, No. 2, pp. 115-119

119

Марија Д. РАДМИЛОВИЋ-РАЂЕНОВИЋ,
Петар Д. БЕЛИЧЕВ, Бранислав М. РАЂЕНОВИЋ

**ИСТРАЖИВАЊЕ МУЛТИПАКТОРСКОГ ЕФЕКТА КОД
СУПЕРПРОВОДНИХ РАДИОФРЕКВЕНТНИХ РЕЗОНАТОРА**

У раду је спроведена анализа мултипакторског ефекта применом једнодимензионалног кода (Particle-in-Cell/Monte Carlo) за симулацију колизионих процеса. Мултипакторски ефекат се појављује када електрон приликом судара са електродом резонатора генерише, у средњем, више од једног секундарног електрона. Однос броја примарних и секундарних електрона дат је преко приноса секундарне емисије. У приказаној анализи коришћен је Штернгласов модел секундарне емисије који укључује енергетску зависност. Добијени резултати показују линеарну зависност времена пробоја од притиска гаса. Показује се такође да број електрона расте у времену док њихова средња енергија опада. Имајући у виду важност секундарне емисије електрона са површина резонатора, приказани резултати могу бити од помоћи у предикцији и елиминисању појаве мултипакторског ефекта приликом пројектовања радиофреквентних резонатора.

Кључне речи: RF резонатор, ефекат мултипликације, секундарна електронска емисија